Exact solutions for some unsteady flows of a couple stress fluid between parallel plates

Article *in* Ain Shams Engineering Journal · June 2016

DOI: 10.1016/j.asej.2016.05.008

CITATIONS
14

READS
1,518

2 authors:

Shehraz Akhtar
Khawaja Fareed University of Engineering & Information Technology,
14 PUBLICATIONS **102** CITATIONS
SEE PROFILE

Nehad Ali Shah
Sejong University
123 PUBLICATIONS **1,298** CITATIONS
SEE PROFILE

Ain Shams Engineering Journal (2018) 9, 985–992

Ain Shams University

Ain Shams Engineering Journal

www.elsevier.com/locate/asej
www.sciencedirect.com

ENGINEERING PHYSICS AND MATHEMATICS

Exact solutions for some unsteady flows of a couple stress fluid between parallel plates

Shehraz Akhtar *, **Nehad Ali Shah**

Abdus Salam School of Mathematical Sciences, GC University Lahore, Pakistan

Received 4 January 2016; revised 24 May 2016; accepted 29 May 2016
Available online 25 June 2016

KEYWORDS

Couple stress fluid;
Unsteady Couette flow;
Unsteady generalized Couette flow;
Unsteady Poiseuille flow

Abstract Exact solutions for three fundamental unsteady flows of an incompressible couple stress fluid between two parallel plates, namely, Couette, generalized Couette and Poiseuille flows, are obtained. Analytical solutions of the corresponding initial-boundary value problems are obtained by means of the integral transforms method (Laplace and finite sine Fourier transforms). For each flow type, the solution is written as the sum between the post transient solution (steady-state solution) and the transient solution. The volume flow rate and skin friction coefficients are, also, obtained. The effect of various parameters on the fluid velocity is graphically underlined and discussed and the critical time to reach the steady-state is also determined.

1. Introduction

Couple stress fluid theory, developed by Stokes [1], is one among the polar fluid theories which considers couple stresses in addition to the classical Cauchy stress. It is the simplest generalization of the classical theory of fluids which allows for polar effects such as the presence of couple stresses and body couples.

This fluid theory is discussed in detail by Stokes in his treatise Theories of Fluids with Microstructure [2] wherein he also presented a list of problems discussed by researchers with reference to this theory.

The couple stress fluids adequately describe the flow behavior of fluid containing a substructure such as lubricants with polymer additives, animal blood, liquid crystals [2].

The importance of couple stress fluids in modern technologies and industries has led the researchers to attempt various problems related to such fluids. Devakar et al. [3] studied some fundamental steady flows of couple stress fluid, namely, Couette, Poiseuille and generalized Couette flows between parallel plates with slip on the boundary.

The flow of couple stress fluids between two moving parallel plates due to a constant pressure gradient was studied by Devakar and Iyengar [4]. MHD free convection flow of couple stress fluids in a vertical porous layer has been studied by Sreenadh et al. [5], by employing the perturbation technique.

Steady Poiseuille flow and heat transfer of couple stress fluids between two parallel inclined plates with variable viscosity are studied by Farooq et al. [6], by means of the perturbation technique. A numerical study of the unsteady MHD flow and

* Corresponding author. Cell: +92 321 6811770.
E-mail addresses: shahraz5768@gmail.com (S. Akhtar), nehadali199@yahoo.com (N.A. Shah).
Peer review under responsibility of Ain Shams University.

Production and hosting by Elsevier

http://dx.doi.org/10.1016/j.asej.2016.05.008

heat transfer of couple stress fluid over a rotating disk was made by Khan et al. [7]. By using a homotopic approach, Hayat et al. [8] investigated the nonlinear unsteady three-dimensional flow of couple stress fluid over a stretched surface in presence of mass transfer and chemical reaction. Some exact solutions for the equations governing the unsteady plane flow of an incompressible couple stress fluid were determined by Naeem [9] using a canonical transformation. Ahmed et al. [10], using complex variables, have studied the oscillatory flows of a couple stress fluid in an inclined, rotating channel. Unsteady magnetohydrodynamic flow of couple stress fluids through a porous medium, between two parallel plates under the influence of pulsating pressure gradient was analyzed by Sarojini et al. [11]. An analytical study of the unsteady hydromagnetic generalized Couette flows of a couple stress fluid, between two parallel plates, under the influence of a periodic body acceleration and pulsating pressure gradient was made by Sulochana [12].

Adesania and Makinde [13] have studied the heat transfer to magnetohydrodynamic non-Newtonian Couple-stress pulsatile flow between two parallel porous plates. The entropy generation in couple-stress fluids flow through porous media was investigated by Makinde and Eegunjobi [14], Adesanya and Makinde [15]. Many interesting problems regarding the couple stress fluids or micropolar fluids can be found in the references [16–21].

In the present paper, we examine the unsteady flow of an incompressible couple stress fluid between two infinite rigid parallel plates. The bottom plate has a translational motion with constant velocity in its plane and the upper plate is fixed. The first studied problem is the generalized Couette flow generated by the lower plate motion and a constant pressure gradient applied in the flow direction. The plane Couette flow was obtained as a particular case. The second problem refers to the Poiseuille flow in which both plates are fixed and the fluid motion is generated by a constant pressure gradient. In all problems the no-slip conditions on the boundaries are considered. By combining the Laplace transform with respect to the temporal variable t, with the finite sine-Fourier transform with respect to the space-variable y, we presented an elegant way to obtain the solution of the governing equation. It is important to point out that, by some manipulations of the inverse Laplace and Fourier transforms, we have written fluid velocity as the sum between the steady-solution and the transient solution. Analyzing the transient solution one can determine the critical time at which the steady-state flow is attained. The volume flow rate and skin friction coefficient on the lower/upper plate were determined. Also, numerical calculations were carried out in order to study the influence of material parameters on the fluid behavior. Some results are illustrated by graphical representations.

2. Problems formulation and solutions

The equations governing the flow of an incompressible couple stress fluid, in the absence of body couples, are given by 2

$$\nabla \cdot \bar{q} = 0, \tag{1}$$

$$\rho \frac{d\bar{q}}{dt} = \rho \bar{f} - \nabla p - \mu \nabla \times \nabla \times \bar{q} - \eta \nabla \times \nabla \times \nabla \times \nabla \times \bar{q}. \tag{2}$$

where ρ is the fluid density, $\bar{q}$ is the velocity vector, $\bar{f}$ is the body force vector, p is the pressure, μ is the dynamic viscosity and η is the couple stress parameter.

For unidirectional unsteady flow between parallel plates, the velocity field $\bar{q} = (u(y,t), 0, 0)$ satisfies the continuity Eq. (1). The momentum Eq. (2) governing the flow, in the absence of body forces, reduces to

$$\rho \frac{\partial u}{\partial t} = -\frac{\partial p}{\partial x} + \mu \frac{\partial^2 u}{\partial y^2} - \eta \frac{\partial^4 u}{\partial y^4}. \tag{3}$$

2.1. Generalized Couette flow

Consider the unsteady laminar flow of an incompressible couple stress fluid between two infinite horizontal parallel plates distance h apart. The upper plate is at rest and lower plate is moving with a constant velocity U. Additionally, a constant pressure gradient G is applied simultaneously in the x-direction (see Fig. 1).

With these assumptions the governing equation is

$$\rho \frac{\partial u}{\partial t} = G + \mu \frac{\partial^2 u}{\partial y^2} - \eta \frac{\partial^4 u}{\partial y^4}. \tag{4}$$

The appropriate initial and boundary conditions are

$$u(y,0) = 0, \quad \text{at} \quad 0 \leqslant y \leqslant h, \tag{5}$$

$$u(0,t) = U, \quad u(h,t) = 0, \quad \text{at} \quad t > 0, \tag{6}$$

$$\frac{\partial^2 u(y,t)}{\partial y^2} = 0 \quad \text{at} \quad y = 0, \quad y = h. \tag{7}$$

Introducing the following non-dimensional quantities

$$y^* = \frac{y}{l}; \quad u^* = \frac{u}{U}; \quad t^* = \frac{Ut}{l}; \quad l^2 = \frac{\eta}{\mu};$$
$$h^* = \frac{h}{l}; \quad Re = \frac{Ul}{\nu}; \quad \text{and} \quad G^* = \frac{l^2}{\mu U} G, \tag{8}$$

and dropping out the star notation, we obtain the next non-dimensional initial-boundary value problem:

$$Re \frac{\partial u}{\partial t} = G + \frac{\partial^2 u}{\partial y^2} - \frac{\partial^4 u}{\partial y^4}, \tag{9}$$

$$u(y,0) = 0, \quad \text{at} \quad 0 \leqslant y \leqslant h, \tag{10}$$

$$u(0,t) = 1, \quad u(h,t) = 0, \quad \text{at} \quad t > 0, \tag{11}$$

$$\frac{\partial^2 u(y,t)}{\partial y^2} = 0 \quad \text{at} \quad y = 0, \quad y = h. \tag{12}$$

Applying the Laplace transform to Eq. (9) and Eqs. (11) and (12), and using Eq. (10) we get the problem

$$sRe\bar{u}(y,s) = \frac{G}{s} + \frac{\partial^2 \bar{u}(y,s)}{\partial y^2} - \frac{\partial^4 \bar{u}(y,s)}{\partial y^4}, \tag{13}$$

$$\bar{u}(0,s) = \frac{1}{s}, \quad \bar{u}(h,s) = 0, \tag{14}$$

$$\frac{\partial^2 \bar{u}(y,s)}{\partial y^2} = 0 \quad \text{at} \quad y = 0, \quad y = h. \tag{15}$$

Multiplying both sides of Eq. (13) by $sin\left(\frac{n\pi y}{h}\right)$, taking the integration from 0 to h with respect to y and using (14) and (15), we obtain

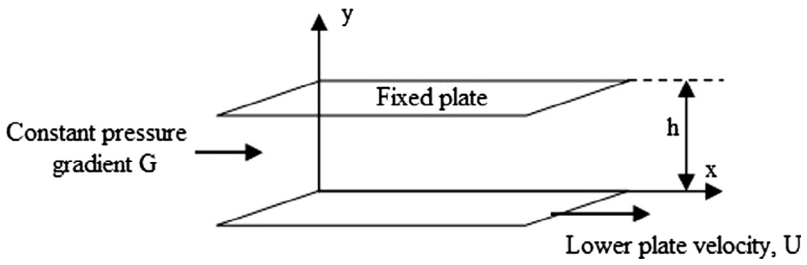

Figure 1 Geometry for generalized Couette flow.

$$\overline{u}_s(n,s)=\frac{G(1-(-1)^n)+\alpha_n^2+\alpha_n^4}{\alpha_n s(sRe+\alpha_n^2+\alpha_n^4)},$$

or equivalently

$$\overline{u}_s(n,s)=\frac{1}{\alpha_n s}+\frac{G(1-(-1)^n)}{\alpha_n^3 s(1+\alpha_n^2)}-\frac{G(1-(-1)^n)}{\alpha_n^3(1+\alpha_n^2)\left(s+\frac{\alpha_n^2+\alpha_n^4}{Re}\right)}-\frac{1}{\alpha_n\left(s+\frac{\alpha_n^2+\alpha_n^4}{Re}\right)}. \quad (16)$$

Applying the Inverse Laplace transform to Eq. (16), we obtain

$$\begin{aligned}u_s(n,t)=&\frac{1-(-1)^n}{\alpha_n}+\frac{(-1)^n}{\alpha_n}-\frac{G(1-(-1)^n)}{\alpha_n}\\&+\frac{G(1-(-1)^n)}{\alpha_n^3}+\frac{G\alpha_n(1-(-1)^n)}{1+\alpha_n^2}\\&-\frac{G(1-(-1)^n)}{\alpha_n^3(1+\alpha_n^2)}e^{-\left(\frac{\alpha_n^2+\alpha_n^4}{Re}\right)t}-\frac{1}{\alpha_n}e^{-\left(\frac{\alpha_n^2+\alpha_n^4}{Re}\right)t}.\end{aligned} \quad (17)$$

Now, applying the inverse sine-Fourier transform to Eq. (17) we obtain [22,23]

$$\begin{aligned}u(y,t)=&1-\frac{y}{h}-G+\frac{Gy(h-y)}{2}\\&+G\left\{\frac{sinh(h-y)+sinh(y)}{sinh(h)}\right\}\\&-\frac{2}{h}\sum_{n=1}^{\infty}\frac{Gsin(\alpha_n y)(1-(-1)^n)}{\alpha_n^3(1+\alpha_n^2)}e^{-\left(\frac{\alpha_n^2+\alpha_n^4}{Re}\right)t}\\&-\frac{2}{h}\sum_{n=1}^{\infty}\frac{sin(\alpha_n y)}{\alpha_n}e^{-\left(\frac{\alpha_n^2+\alpha_n^4}{Re}\right)t},\end{aligned} \quad (18)$$

or, the equivalent form

$$\begin{aligned}u(y,t)=&1-G-\left(\frac{1}{h}-\frac{Gh}{2}\right)y-\frac{G}{2}y^2+G\left\{\frac{cosh\left(\frac{h}{2}-y\right)}{cosh\left(\frac{h}{2}\right)}\right\}\\&-\frac{2}{h}\sum_{n=1}^{\infty}\left(\frac{G(1-(-1)^n)}{\alpha_n^3(1+\alpha_n^2)}+\frac{1}{\alpha_n}\right)sin(\alpha_n y)e^{-\left(\frac{\alpha_n^2+\alpha_n^4}{Re}\right)t}.\end{aligned} \quad (19)$$

Our final solution is the sum between the post-transient (steady) solution and transient solution, with the post-transient (or steady-state) solution

$$u_p(y)=1-G-\left(\frac{1}{h}-\frac{Gh}{2}\right)y-\frac{G}{2}y^2+G\left\{\frac{cosh\left(\frac{h}{2}-y\right)}{cosh\left(\frac{h}{2}\right)}\right\}, \quad (20)$$

and, the transient solution $u_t(y,t)$

$$u_t(y,t)=-\frac{2}{h}\sum_{n=1}^{\infty}\left(\frac{G(1-(-1)^n)}{\alpha_n^3(1+\alpha_n^2)}+\frac{1}{\alpha_n}\right)sin(\alpha_n y)e^{-\left(\frac{\alpha_n^2+\alpha_n^4}{Re}\right)t}. \quad (21)$$

The non-dimensional volume flow rate of the channel is given by

$$\begin{aligned}Q(t)=&\int_0^h u(y,t)dy=\frac{h}{2}-Gh+\frac{Gh^3}{12}+2Gtanh\left(\frac{h}{2}\right)\\&+\frac{4}{h}\sum_{n=0}^{\infty}\left(\frac{2G}{\alpha_{2n+1}^4(1+\alpha_{2n+1}^2)}-\frac{1}{\alpha_{2n+1}^2}\right)e^{-\left(\frac{\alpha_{2n+1}^2+\alpha_{2n+1}^4}{Re}\right)t}.\end{aligned} \quad (22)$$

In order to determine the skin friction coefficients, we recall that, the non-dimensional shear stress is given by

$$\tau_{xy}(y,t)=\frac{\partial u(y,t)}{\partial y}-\frac{\partial^3 u(y,t)}{\partial y^3}. \quad (23)$$

Using Eqs. (19) and (23) we find that the skin friction on the lower plate is

$$\begin{aligned}Cf_{lp}(t)=\tau_{xy}(0,t)=&-\frac{1}{h}+\frac{Gh}{2}-\frac{2}{h}\sum_{n=1}^{\infty}\left(\frac{G(1-(-1)^n)}{\alpha_n^2(1+\alpha_n^2)}+1\right)\\&\times(1+\alpha_n^2)e^{-\left(\frac{\alpha_n^2+\alpha_n^4}{Re}\right)t}\end{aligned} \quad (24)$$

respectively, and the skin friction on the upper plate is

$$\begin{aligned}Cf_{up}(t)=\tau_{xy}(h,t)=&-\frac{1}{h}-\frac{Gh}{2}-\frac{2}{h}\sum_{n=1}^{\infty}(-1)^n\left(\frac{G(1-(-1)^n)}{\alpha_n^2(1+\alpha_n^2)}+1\right)\\&\times(1+\alpha_n^2)e^{-\left(\frac{\alpha_n^2+\alpha_n^4}{Re}\right)t}\end{aligned} \quad (25)$$

Of course, as it was to be expected, the solutions (20)–(25) provide the solutions corresponding to the plane Couette flow ($G=0$).

For this particular flow, the velocity field is given by

$$u(y,t)=u_p(y)+u_t(y.t), \quad (26)$$

with

$$\begin{aligned}u_p(y)=&1-\frac{y}{h},\quad u_t(y,t)\\=&-\frac{2}{h}\sum_{n=1}^{\infty}\frac{sin(\alpha_n y)}{\alpha_n}e^{-\left(\frac{\alpha_n^2+\alpha_n^4}{Re}\right)t}.\end{aligned} \quad (27)$$

The non-dimensional volume flow rate of the channel is given by

$$Q(t)=\int_0^h u(y,t)dy=\frac{h}{2}-\frac{4}{h}\sum_{n=0}^{\infty}\frac{1}{\alpha_{2n+1}^2}e^{-\left(\frac{\alpha_{2n+1}^2+\alpha_{2n+1}^4}{Re}\right)t}, \quad (28)$$

and, the skin friction coefficients are

$$Cf_{lp}(t) = -\frac{1}{h} - \frac{2}{h}\sum_{n=1}^{\infty}(1+\alpha_n^2)e^{-\left(\frac{\alpha_{2n+1}^2+\alpha_{2n+1}^4}{Re}\right)t}$$

$$Cf_{up}(t) = -\frac{1}{h} - \frac{2}{h}\sum_{n=1}^{\infty}(-1)^n(1+\alpha_n^2)e^{-\left(\frac{\alpha_{2n+1}^2+\alpha_{2n+1}^4}{Re}\right)t} \quad (29)$$

2.2. Plane Poiseuille flow

Consider the unsteady laminar flow of an incompressible couple stress fluid between two infinite horizontal parallel plates distance h apart. Both the plates are assumed to be at rest and the flow is due to the constant pressure gradient G in the x-direction.

With these assumptions, the governing equation is given by Eq. (4).

The appropriate initial and boundary conditions are

$$u(y,0) = 0, \quad \text{at} \quad 0 \leqslant y \leqslant h, \quad (30)$$

$$u(0,t) = 0, \quad u(h,t) = 0, \quad \text{at} \quad t > 0, \quad (31)$$

$$\frac{\partial^2 u(y,t)}{\partial y^2} = 0 \quad \text{at} \quad y = 0, \quad y = h. \quad (32)$$

Introducing the following non-dimensional quantities

$$y^* = \frac{y}{l}; \quad u^* = \frac{lu}{v}; \quad t^* = \frac{vt}{l^2}; \quad l^2 = \frac{\eta}{\mu};$$

$$h^* = \frac{h}{l}; \quad \text{and} \quad G^* = \frac{l^3\rho}{\mu^2}G, \quad (33)$$

and dropping out the star notation, we obtain the next non-dimensional initial-boundary value problem:

$$\frac{\partial u}{\partial t} = G + \frac{\partial^2 u}{\partial y^2} - \frac{\partial^4 u}{\partial y^4}, \quad (34)$$

$$u(y,0) = 0, \quad \text{at} \quad 0 \leqslant y \leqslant h, \quad (35)$$

$$u(0,t) = 0, \quad u(h,t) = 0, \quad \text{at} \quad t > 0, \quad (36)$$

$$\frac{\partial^2 u(y,t)}{\partial y^2} = 0 \quad \text{at} \quad y = 0, \quad y = h. \quad (37)$$

Applying the Laplace transform to Eq. (34) and Eqs. (36) and (37), and using (35) we get

$$s\overline{u}(y,s) = \frac{G}{s} + \frac{\partial^2 \overline{u}(y,s)}{\partial y^2} - \frac{\partial^4 \overline{u}(y,s)}{\partial y^4}, \quad (38)$$

$$\overline{u}(0,s) = 0, \quad \overline{u}(h,s) = 0, \quad (39)$$

$$\frac{\partial^2 \overline{u}(y,s)}{\partial y^2} = 0 \quad \text{at} \quad y = 0, \quad y = h. \quad (40)$$

By using the same way as in previous case, we obtain

$$\overline{u}_s(n,s) = \frac{G(1-(-1)^n)}{\alpha_n s(s+\alpha_n^2+\alpha_n^4)},$$

or equivalently

$$\overline{u}_s(n,s) = \frac{G(1-(-1)^n)}{\alpha_n^3 s(1+\alpha_n^2)} - \frac{G(1-(-1)^n)}{\alpha_n^3(1+\alpha_n^2)(s+\alpha_n^2+\alpha_n^4)}. \quad (41)$$

Applying the inverse Laplace transform to Eq. (41), we get

$$u_s(n,t) = \frac{G(1-(-1)^n)}{\alpha_n^3(1+\alpha_n^2)} - \frac{G(1-(-1)^n)}{\alpha_n^3(1+\alpha_n^2)}e^{-(\alpha_n^2+\alpha_n^4)t},$$

or equivalently

$$u_s(n,t) = -\frac{G(1-(-1)^n)}{\alpha_n} + \frac{G(1-(-1)^n)}{\alpha_n^3} + \frac{G\alpha_n(1-(-1)^n)}{1+\alpha_n^2} - \frac{G(1-(-1)^n)}{\alpha_n^3(1+\alpha_n^2)}e^{-(\alpha_n^2+\alpha_n^4)t}. \quad (42)$$

Applying the inverse sine-Fourier transform to Eq. (42), we obtain [22,23]

$$u(y,t) = -G + \frac{Gy(h-y)}{2} + G\left\{\frac{sinh(h-y)+sinh(y)}{sinh(h)}\right\} - \frac{2}{h}\sum_{n=1}^{\infty}\frac{Gsin(\alpha_n y)(1-(-1)^n)}{\alpha_n^3(1+\alpha_n^2)}e^{-(\alpha_n^2+\alpha_n^4)t}, \quad (43)$$

which can be written as

$$u(y,t) = -G + \frac{Gh}{2}y - \frac{G}{2}y^2 + G\left\{\frac{cosh\left(\frac{h}{2}-y\right)}{cosh\left(\frac{h}{2}\right)}\right\} - \frac{4}{h}\sum_{n=0}^{\infty}\frac{G}{\alpha_{2n+1}^3\left(1+\alpha_{2n+1}^2\right)}sin(\alpha_{2n+1}y)e^{-\left(\alpha_{2n+1}^2+\alpha_{2n+1}^4\right)t}. \quad (44)$$

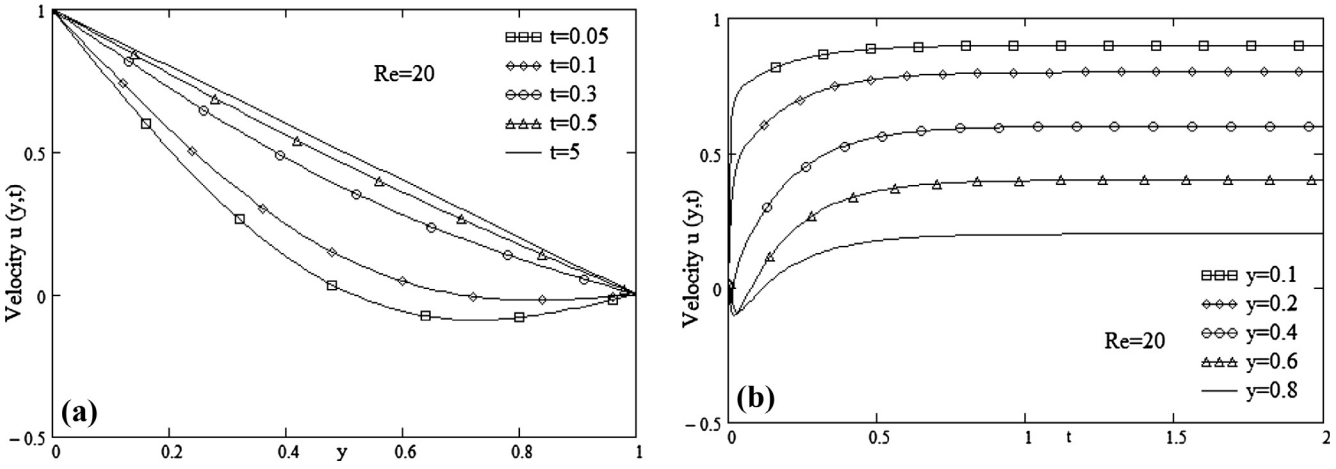

Figure 2 Plane Couette flow velocity profiles.

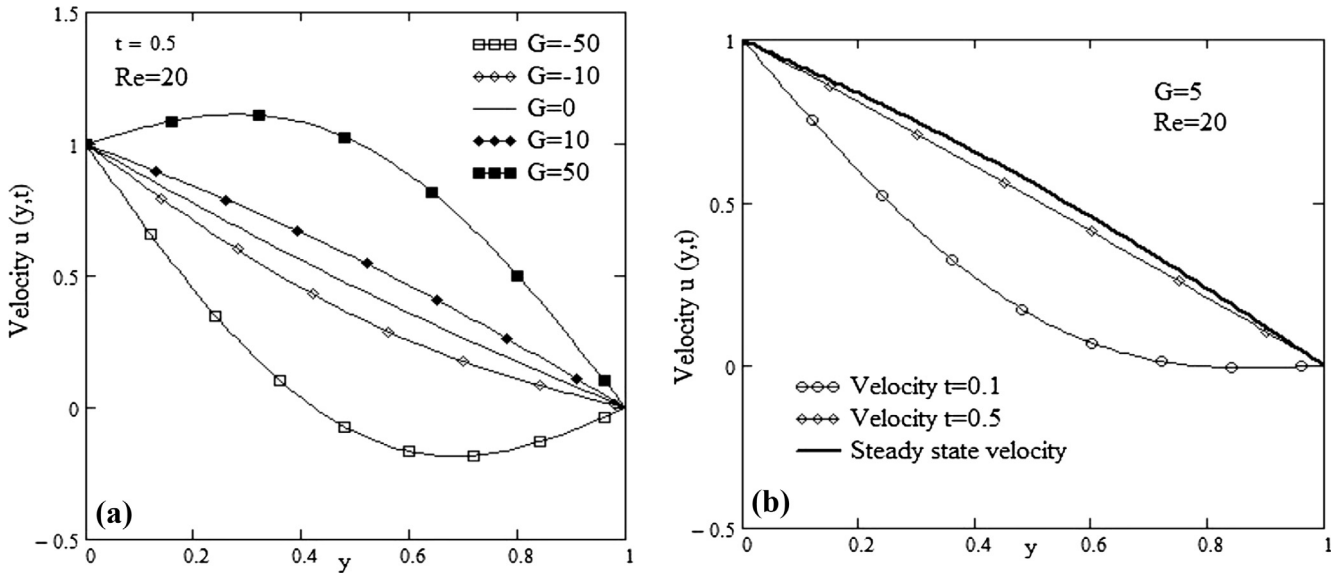

Figure 3 Generalized Couette flow velocity profiles.

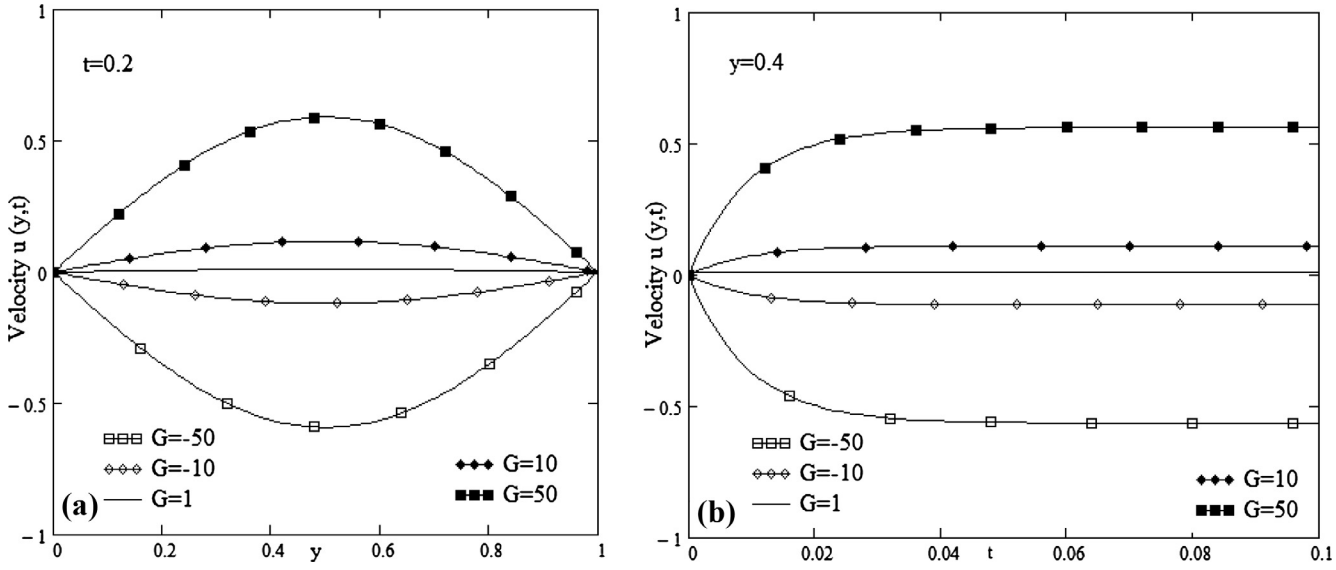

Figure 4 Plane Poiseuille flow profiles.

Our final solution is the sum between the post-transient (steady) solution and transient solution, with the post-transient (or steady-state) solution

$$u_p(y,t) = -G + \frac{Gh}{2}y - \frac{G}{2}y^2 + G\left\{\frac{cosh\left(\frac{h}{2}-y\right)}{cosh\left(\frac{h}{2}\right)}\right\}, \tag{45}$$

and, transient solution $u_t(y,t)$

$$u_t(y,t) = -\frac{4}{h}\sum_{n=0}^{\infty}\frac{G}{\alpha_{2n+1}^3\left(1+\alpha_{2n+1}^2\right)}sin(\alpha_{2n+1}y)e^{-\left(\alpha_{2n+1}^2+\alpha_{2n+1}^4\right)t}. \tag{46}$$

The non-dimensional volume flow rate of the channel is given by

$$\begin{aligned} Q(t) &= \int_0^h u(y,t)dy \\ &= -Gh + \frac{Gh^3}{12} + 2Gtanh\left(\frac{h}{2}\right) \\ &\quad + \frac{8}{h}\sum_{n=0}^{\infty}\frac{Ge^{-\left(\alpha_{2n+1}^2+\alpha_{2n+1}^4\right)t}}{\alpha_{2n+1}^4\left(1+\alpha_{2n+1}^2\right)}. \end{aligned} \tag{47}$$

Similar to previous case, we obtain the skin friction coefficients as

$$Cf_{lp}(t) = \frac{Gh}{2} - \frac{4}{h}\sum_{n=0}^{\infty}\frac{G}{\alpha_{2n+1}^2}e^{-\left(\alpha_{2n+1}^2+\alpha_{2n+1}^4\right)t} \quad Cf_{up}(t) = -Cf_{lp}(t) \tag{48}$$

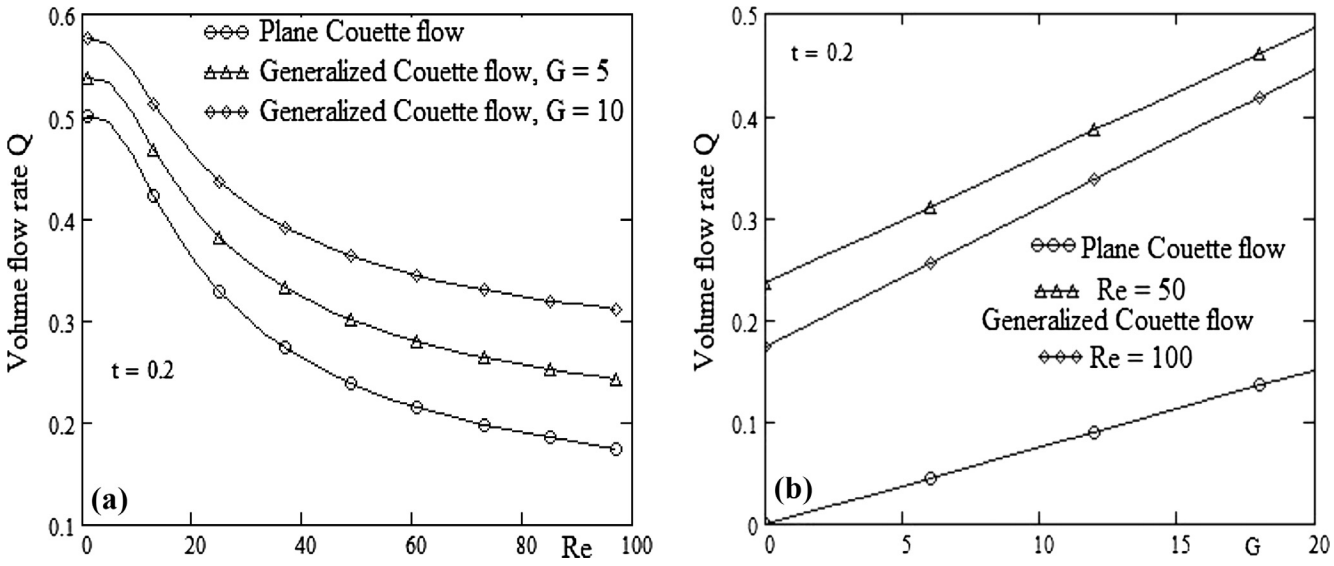

Figure 5 Profiles of the volume flow rate.

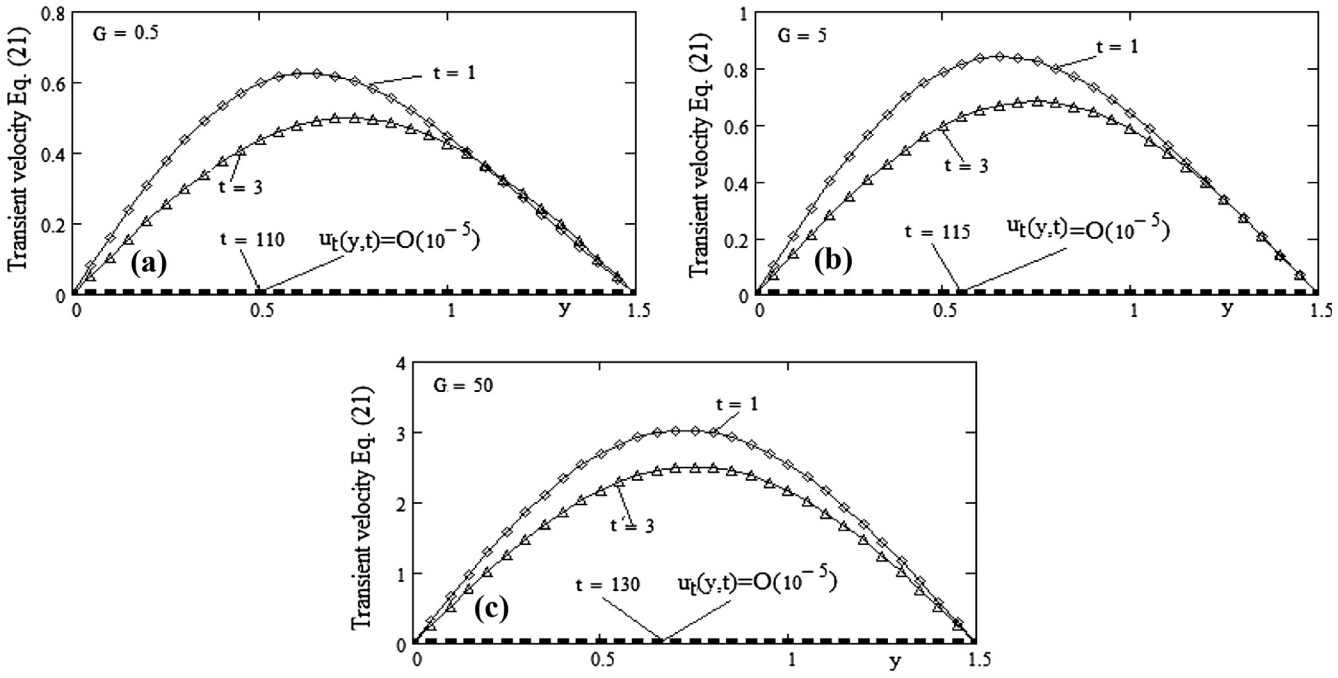

Figure 6 Decrease of the transient solution for generalized Couette flows.

3. Results and discussion

The numerical values of the velocity, volume flow rate and skin friction coefficient are computed for different parameters such as Reynolds number Re and non-dimensional pressure gradient G. In all numerical simulations we used $n = 200$ terms in the series solutions. For this approximate solution, the absolute error is of order 10^{-6}.

Profiles of the velocity $u(y,t)$ of the plane Couette flow, given by Eq. (26) are plotted in Fig. 2a and b for $Re = 20$ and $h = 1$. In Fig. 2a, the profiles of the velocity $u(y,t)$ are sketched versus the variable y for different values of the time t. It is observed from this figure that, for lower values of the time t velocity decreases to attain a minimum negative value and after it increases to be zero on the upper plate. One must note that this behavior is only for a short time interval ($t \leqslant 0.2$ in the studied case). Because the exponential function tends fast to zero, the steady-state of plane Couette flow is attained at small value of the time t. Fig. 2b shows the diagrams of the velocity for several values of the spatial coordinate y. Obviously, the results are in good agreement with those shown in Fig. 2a, namely, for small values of the time t and large values of y variable, the reverse flow appears (see curves corresponding to $y = 0.6$ and $y = 0.8$ from Fig. 2b). For increasing values of y, the velocity decreases and, for large values of the time t, velocity becomes constant.

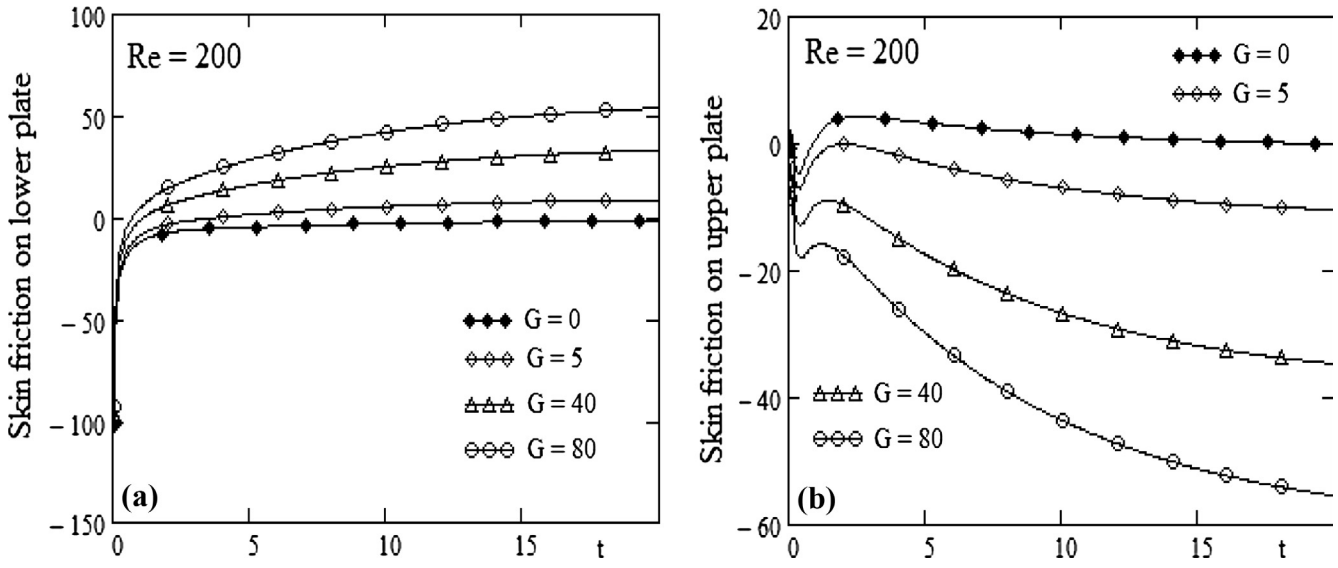

Figure 7 Skin friction profiles for Couette and generalized Couette flows.

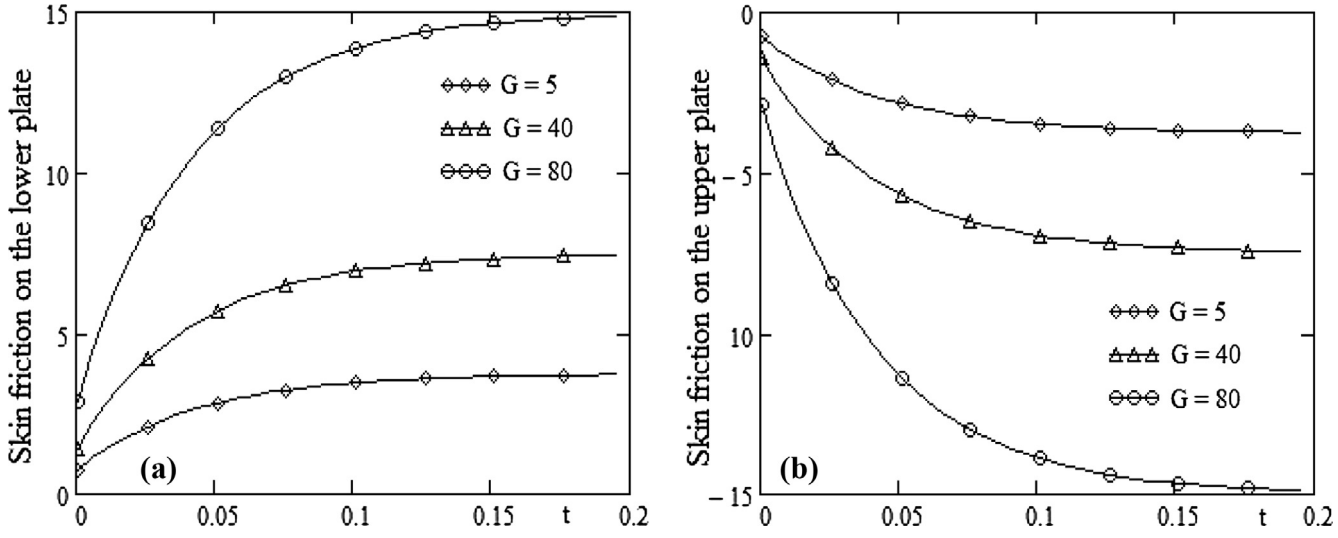

Figure 8 Skin friction profiles for plane Poiseuille flows.

Profiles of the velocity $u(y,t)$, given by Eq. (19) corresponding to the generalized Couette flow are presented in Fig. 3a and b, for $Re = 20$ and $h = 1$. Fig. 3a shows variation of the velocity $u(y,t)$ versus y for $t = 0.5$ and several values of the pressure gradient G. The curve corresponding to $G = 0$ represents the velocity for Couette flow. For positive and increasing values of the pressure gradient, values of the velocity $u(y,t)$ are increasing. For negative values of the parameter G, the fluid flows in an opposite sense to the x-axis. In Fig. 3b, we compared the starting solution $u(y,t)$ with the steady-state solution, for $G = 5$. It is easy to see that, values of the function $u(y,t)$ approach to the values of steady-state function for increasing values of time t.

Fig. 4 was drawn in order to study the velocity of the Poiseuille flow. Into Fig. 4a are plotted the curves corresponding to the velocity $u(y,t)$ given by Eq. (43). The curves are depicted versus y, for $t = 0.2$. It is observed that, the flow is symmetric with respect to middle of channel and, in absolute value, the fluid velocity increases for increasing values of the parameter G. The curves from Fig. 4b are plotted with respect to time t, for $y = 0.4$. For lower values of the time t, the fluid velocity increases in absolute value and tends to a constant value for fixed y. Therefore, the influence of the transient solution is significant only for small values of the time t.

In Fig. 5 are depicted the curves corresponding to the volume flow rate at the moment $t = 0.2$. These curves are sketched versus Reynolds number Re(Fig. 5a) and, versus parameter G(Fig. 5b). As expected, the volume flow rate increases with the pressure gradient G. The Reynolds number has an opposite effect for Couette and generalized Couette flows, namely, the volume flow rate decreases with increasing values of the Reynolds number.

In order to determine the critical time at which the steady state is attained, we have carried out numerical calculations

with the transient solutions (21), (27) and (46). From the numerical simulations, we have obtained that, for plane Couette flows the transient part has a little contribution only if the Reynolds number has very large values.

Similarly, for Poiseuille flows, the transient part has insignificant contribution. In both cases it can observe that the exponential functions tend to zero for small values of the time t. For generalized Couette flow the transient part has a significant contribution as it can be seen from Fig. 6. Comparing the absolute value of the transient solution given by Eq. (21), at different values of the time t, we obtain that the required time, to attain the steady flows increases if the couple-stress parameter increases (or equivalent, the non-dimensional parameter G increases. See Eq. (8)). Curves from Fig. 6 are depicted for $h = 1.5$ and $Re = 250$.

Figs. 7 and 8 present the skin friction on the lower and upper plate for the Couette and generalized Couette flows (Fig. 7), respectively, for the generalized Couette flow and plane Poiseuille flow (Fig. 8), for $h = 1.5$ and $Re = 200$. It must be noted that, in all cases, the absolute values of shear stresses on plate increase with the parameter G.

Acknowledgements

The authors are thankful to Abdus Salam School of Mathematical Sciences, GC University, Lahore, Pakistan, for the support and facilitating the research work. They also would like to express their gratitude to referees for both careful assessment and fruitful comments and suggestions regarding the manuscript.

References

[1] Stokes VK. Couple stress in fluid. Phys Fluids 1966;9:1709–15.
[2] Stokes VK. Theories of fluids with microstructure. New York: Springer; 1984.
[3] Devakar M, Sreenivasu D, Shankar B. Analytical solutions of couple stress fluid flows with slip boundary conditions. Alexandria Eng J 2014;53:723–30.
[4] Devakar M, Iyengar TKV. Run up flow of a couple stress fluid between parallel plates. Nonlinear Anal: Modell Control 2010;15 (1):29–37.
[5] Sreenadh S, Kishore SN, Srinivas ANS, Reddy RH. MHD free convection flow of couple stress fluid in a vertical porous layer. Adv Appl Sci Res 2011;2(6):215–22.
[6] Farooq M, Rahim MT, Islam S, Siddiqui AM. Steady Poiseuille flow and heat transfer of couple stress fluids between two parallel inclined plates with variable viscosity. J Assoc Arab Univ Basic Appl Sci 2013;14:9–18.
[7] Khan NA, Aziz S, Khan NA. Numerical simulation for the unsteady MHD flow and heat transfer of couple stress fluid over a rotating disk. PLoS ONE 2014;9(5):e95432. http://dx.doi.org/10.1371/journal.pone.0095423.
[8] Hayat T, Awais M, Safdar A, Hendi AA. Unsteady three dimensional flow of couple stress fluid over a stretched surface with chemical reaction. Nonlinear Anal: Modell Control 2012;17 (1):47–59.
[9] Naeem RK. Some new exact solutions to unsteady flow equations of incompressible couple stress fluid. Int J Appl Math Mech 2010;6(15):1–11.
[10] Ahmed S, Beg OA, Ghosh SK. A couple stress fluid modeling on free convection oscillatory hydromagnetic flow in an inclined rotating channel. Ain Shams Eng J 2014;5:1249–65.
[11] Sarojini MS, Krishna MV, Shankar CU. Unsteady MHD flow of a couple stress fluid through a porous medium, between parallel plates under the influence of pulsating pressure gradient. Int J Sci Eng Res 2012;3(4):1–6.
[12] Sulochana P. Unsteady MHD pulsatile flow of couple stress fluid under the influence of periodic body acceleration between parallel plates. Adv Appl Sci Res 2014;5(4):136–43.
[13] Adesanya SO, Makinde OD. Heat transfer to magnetohydrodynamic non-Newtonian couple stress pulsatile flow between two parallel porous plates. Z Naturforsch 2012;67a:647–56.
[14] Makinde OD, Eegunjobi AS. Entropy generation in a couple stress fluid flow through a vertical channel filled with saturated porous media. Entropy 2013;15:4589–606.
[15] Adesanya SO, Makinde OD. Entropy generation in couple stress fluid flow through porous channel with fluid slippage. Int J Exergy 2014;15(3):344–62.
[16] Adesanya SO, Makinde OD. Effects of couple stresses on entropy generation rate in a porous channel with convective heating. Comput Appl Math 2015;34:293–307.
[17] Adesanya SO, Makinde OD. Irreversibility analysis in a couple stress film flow along an inclined heated plate with adiabatic free surface. Phys A: Stat Mech Appl 2015;432:222–9.
[18] Naduvinamani NB, Fathima ST, Hiremath PS. Effect of surface roughness on characteristics of couple stress squeeze film between anisotropic porous rectangular plates. Fluid Dyn. Res. 2003;32 (5):217–31.
[19] Lin JR, Hung CR. Combined effects of non-Newtonian couple stress and fluid inertia on the squeeze film characteristics between a long cylinder and an infinite plate. Fluid Dyn. Res. 2007;39 (8):616–39.
[20] Naduvinamani NB, Hiremath PS, Gurubasavaraj G. Effects of surface roughness on couple stress squeeze film between a sphere and a flat plate. Tribol. Int. 2005;38:451–8.
[21] Ashmawy lA. Unsteady Couette flow of a micropolar fluid with slip. Meccanica 2012;47:85–94.
[22] Debnath L, Bhatta D. Integral transforms and their applications. 2nd ed. Chapman and Hall/C.R.C.; 2006.
[23] Gradshteyn IS, Ryzhik IM. Table of integrals, series, and products. 7th ed. Elsevier Academic Press Publications; 2007.